

# Experiments in Fundamental Physics scheduled and in development for the ISS

C. Lämmerzahl<sup>1</sup>, G. Ahlers<sup>2</sup>, N. Ashby<sup>3</sup>, M. Barmatz<sup>4</sup>, P.L. Biermann<sup>5</sup>, H. Dittus<sup>1</sup>, V. Dohm<sup>6</sup>, R. Duncan<sup>7</sup>, K. Gibble<sup>8</sup>, J. Lipa<sup>9</sup>, N. Lockerbie<sup>10</sup>, N. Mulders<sup>11</sup>, C. Salomon<sup>12</sup>

<sup>1</sup> ZARM, University Bremen, Am Fallturm, 28359 Bremen, Germany

<sup>2</sup> iQUEST and Department of Physics, University of California, Santa Barbara, CA 93106, USA

<sup>3</sup> Physics Department, University of Colorado at Boulder, Boulder, CO 80309, USA

<sup>4</sup> Jet Propulsion Laboratory, California Institute of Technology, Pasadena, California 91109-8099, USA

<sup>5</sup> Max-Planck-Institute for Radio Astronomy, Auf dem Hügel 69, 53121 Bonn, Germany

<sup>6</sup> Institute for Theoretical Physics, Aachen University, 52056 Aachen, Germany

<sup>7</sup> University of New Mexico, Albuquerque, NM 87131, USA

<sup>8</sup> Department of Physics, Penn State University University Park, PA 16802, USA

<sup>9</sup> Physics Department, Stanford University, Stanford, CA 94305-4085, USA

<sup>10</sup> University of Strathclyde, Department of Physics and Applied Physics, Glasgow G40NG, Scotland

<sup>11</sup> Department of Physics and Astronomy, University of Delaware, Newark, DE 19716, USA

<sup>12</sup> Département de physique de l'Ecole Normale Supérieure, Laboratoire Kastler Brossel, 24 rue Lhomond, 75231 Paris, France

**Abstract:** This is a review of those experiments in the area of Fundamental Physics that are either approved by ESA and NASA, or are currently under development, which are to be performed in the microgravity environment of the International Space Station. These experiments cover the physics of liquid Helium (SUE, BEST, MISTE, DYNAMX, and EXACT), ultrastable atomic clocks (PHARAO, PARCS, RACE), ultrastable microwave resonators (SUMO), and particle detectors (AMS and EUSO). The scientific goals are to study more precisely the universality properties of liquid He under microgravity conditions, to establish better time standards and to test the universality of the gravitational red shift, to make more precise tests of the constancy of the speed of light, and to measure the particle content in space directly without disturbances from the Earth's inner atmosphere.

## *Introduction*

**Fundamental Physics:** The area of today's Fundamental Physics can be divided broadly into two categories of theories: Universal theories like Quantum Theory, and Special and General Relativity, and the universal theories of many-particle systems such as the Renormalization-Group theory, and Physical theories like the theory of gravity and the electromagnetic interaction, or the standard model of elementary particle physics. The universal theories are

- Quantum Theory [characterized by Planck's constant  $\hbar$ ]

- Special Relativity [characterized by the velocity of light  $c$ ]
- General Relativity [characterized by  $\kappa = G/c^2$ , where  $G$  is Newton's gravitational constant]
- Many particle (or statistical) physics [characterized by the Boltzmann constant  $k_B$ ]

and the theories dealing with the four interactions are

- Gravitational interaction [characterized by Newton's constant  $G$ ]
- Electromagnetic interaction [characterized by the fine structure constant,  $\alpha$ ]
- Weak interaction [characterized by  $\alpha_{\text{weak}}$ ]
- Strong interaction [characterized by  $\alpha_{\text{strong}}$ ]

These theories represent our knowledge about all physical phenomena, from the evolution of the Universe and the creation of galaxies and planetary systems, to the functioning of everyday devices like cars, computers, positioning systems, etc.

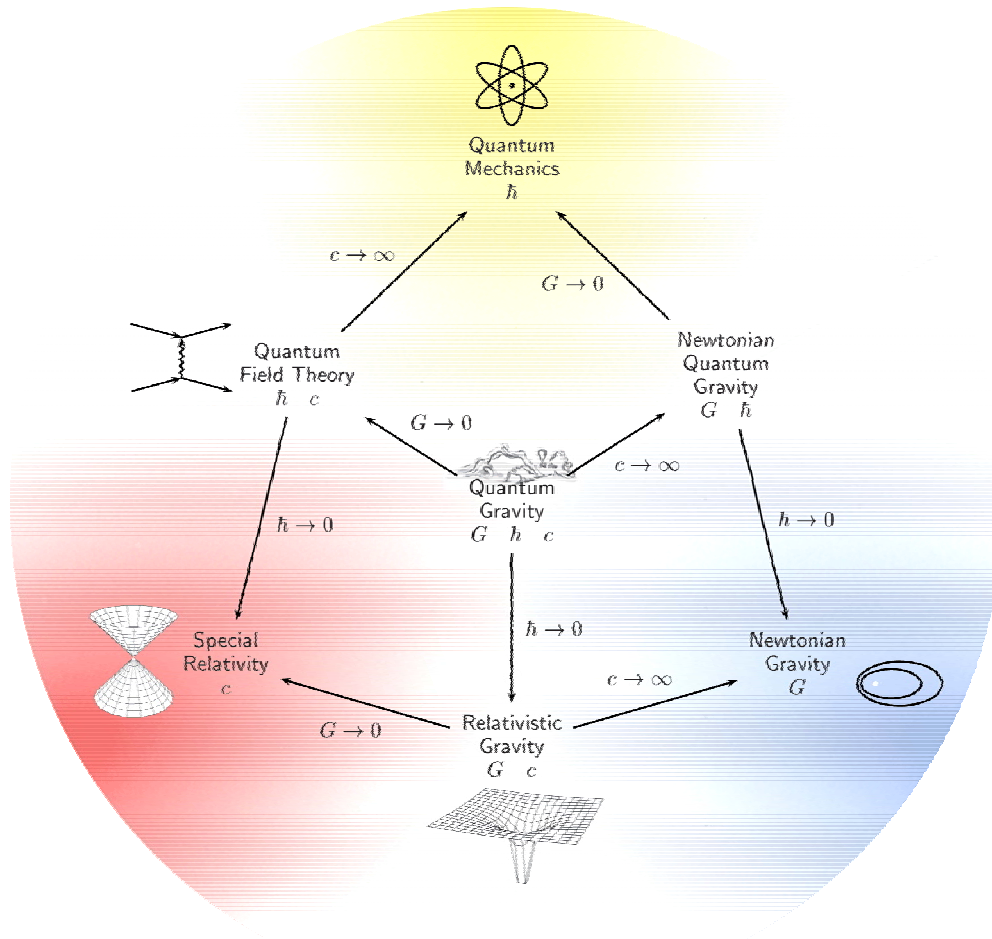


**Fig.1:** The relations between Fundamental Theories as characterized by the fundamental constants.

**Important problems in Fundamental Physics:** As can be seen from the list of interactions gravity plays a double role both as a universal theory and as a particular interaction, which is certainly one reason for the difficulty encountered so far in quantizing gravity or unifying it with the other interactions. In fact the most outstanding problem in the first category is the incompatibility of quantum theory and gravity. Some examples where the present notion of physics breaks down are the information loss in black holes, the nature of singularities, and the ‘big bang’. This implies the need for a unified physical description, that is, a theory of quantum gravity. The current approaches towards this goal are string theory and the canonical quantization of gravity or loop gravity (see [1] for a recent review). Here, string theory also offers the possibility of unifying all interactions, a wish that is connected with the second category of theories mentioned above. Good reasons in favour of such a unification procedure are the universality principles which Special and General Relativity are based upon, that is to say the Relativity principle, the Universality of free fall (also called Weak equivalence principle) and the Universality of the gravitational redshift (also called Local Position Invariance, or LPI). However, approaches to quantum gravity such as string theory predict tiny violations of these universality principles, and thus small violations of Special and General Relativity which are, in this approach, valid only in the low energy limit<sup>1</sup>.

With regard to many-particle physics a fascinating problem is the understanding of the organizing principles that are established in condensed matter systems, for example the spontaneous formation of long-range order below a sharply defined critical temperature. Here, Renormalization-Group (RG) theory [4] plays a fundamental role as it predicts universal behaviour under various different physical conditions. The RG theory has not only explained a wide range of experimental results in critical phenomena, but the RG concept has opened up the possibility of solving a significant number of problems that are among the most difficult in theoretical physics. Successful applications of the RG approach range from statistical physics to hydrodynamics, solid state physics to elementary particle physics, and even to problems in quantum gravity. For these reasons, a highly precise experimental test of the RG predictions is of fundamental interest. The most outstanding RG predictions are the features of universality and scaling near critical points of vastly different condensed matter systems (fluids, alloys, magnetic materials, superfluids, superconductors, fluid mixtures, etc.).

All of the foregoing remarks make it clear that the future development of physics really needs improved experimental data; and one way of achieving this is to make use of microgravity conditions.

Many of the fundamental experimental tests are experiments on (i) the constancy of the speed of light, that is, they analyse a hypothetical dependency of the velocity of light of the form

$$c = c(\mathcal{G}, v) \tag{0.1}$$

on the orientation  $\mathcal{G}$  and/or the velocity  $v$  of the laboratory, and (ii) testing the gravitational red shift, that is, the frequency difference between clocks located at different position  $x_1$  and  $x_2$  in the gravitational field, usually expressed in the form

---

<sup>1</sup> More on this and related questions can be found in [2]. See also the article of G. Amelino-Camelia [3] in this issue.

$$\nu(x_2) = \left(1 - \frac{U(x_2) - U(x_1)}{c^2}\right) \nu(x_1),$$

where  $\nu(x)$  is the frequency of the clock at position  $x$  and  $U$  is the Newtonian gravitational potential. If this red shift depends on the clock, then

$$\nu(x_2) = \left(1 + \alpha_{clock} \frac{U(x_1) - U(x_2)}{c^2}\right) \nu(x_1)$$

and a comparison between the frequencies of two different clocks will give

$$\frac{\nu_{clock_A}(x_2)}{\nu_{clock_B}(x_2)} = \left(1 - (\alpha_{clock_A} - \alpha_{clock_B}) \frac{U(x_2) - U(x_1)}{c^2}\right) \frac{\nu_{clock_A}(x_1)}{\nu_{clock_B}(x_1)} \quad (0.2)$$

so that the ratio of the frequencies of two clocks will vary with the position proportional to the gravitational potential difference with the coefficient  $\alpha_{AB} = \alpha_{clock_A} - \alpha_{clock_B}$ . Eqs.(0.1) and (0.2) are the basis for the tests of Special Relativity and of the Universality of the gravitational red shift, which together with the Universality of free fall forms the Einstein Equivalence Principle which is the basis of any metrical theory of gravity [5] as the Einstein gravitational theory is. String theory, for example, predicts that  $\alpha_{AB} \neq 0$  in general, see e.g. [6]. — It is also clear that the better clocks needed for these improved tests also contribute to a better time standard and thus to metrology, and to the GPS.

As far as important tests in RG theory are concerned, we mention briefly three examples: (i) Critical points are characterized by a divergent correlation length  $\xi$  and by singularities of the temperature dependence of thermodynamic quantities, e.g. a singular specific heat  $C$ , according to

$$\xi = \xi_0^\pm |t|^{-\nu}, \quad C = A^\pm |t|^{-\alpha}, \quad (0.3)$$

where  $t = (T - T_c)/T_c$  is the relative temperature distance from  $T_c$  and where + and – refer to  $T > T_c$  and  $T < T_c$ , respectively. The critical exponents  $\nu$  and  $\alpha$  as well as the amplitude ratios  $\xi_0^+/\xi_0^-$  and  $A^+/A^-$  are predicted to be universal, i.e., independent of the details of the microscopic interaction [7]. Furthermore there exist exact relations between the various critical exponents, for example

$$2 - \alpha = 3\nu. \quad (0.4)$$

To test the correctness of these predictions constitutes a fundamental test of the correctness of the RG theory in general.

(ii) In a confined geometry of characteristic length  $L$ , there exists the prediction of "finite-size scaling" [8,9] for the specific heat  $C(t, L)$  and for other thermodynamic and dynamic quantities, e.g.,

$$C(t, L) - C(t, \infty) = L^{\alpha/\nu} f(L/\xi), \quad (0.5)$$

where  $\xi$  is the correlation length (0.3). Again, the scaling function  $f(x)$  is predicted to be universal (for a given geometry and boundary conditions). So far, however, there exist strong discrepancies between this prediction and real experiments in confined superfluid Helium [10,11].

(iii) It is of great physical interest to investigate cooperative phenomena in condensed-matter systems under non-equilibrium conditions and in the non-linear response regime. There exist detailed RG predictions in this regime near the superfluid transition of  $^4\text{He}$  in the presence of a heat current [12,13]. An as yet unresolved fun-

damental question is whether there exist hysteresis effects in such non-equilibrium systems [14].

**Fundamental Physics in Microgravity:** A microgravity environment offers important advantages for Fundamental Physics experiments over ground-based laboratories and is even mandatory for some experiments. These advantages could be broken down into basic or intrinsic advantages or requirements (space conditions), and practical experimental requirements

- Infinitely long ‘free fall’ under microgravity conditions.
- Long exposure to very weak interactions is possible, rendering their effects measurable.
- No seismic noise—quiet environmental conditions.
- The cosmic particle content of space itself.
- Huge distances and variations in altitude.
- Large velocities and large velocity variations.
- Large potential differences may be used.

One of the most powerful arguments for the utilization of the ISS for Fundamental Physics experimentation is the unrivalled opportunity for quicker, easier, and repeatable access to the experimental apparatus for adjustment, repair, repetition of experiments, a post-mission analysis of the apparatus — something that is quite impossible in the case of dedicated satellites. In consequence, this facility must reduce considerably the time-scales and costs associated with the practical realisation of such experiments.

**This review:** In this paper we review the current Fundamental physics projects planned to be performed onboard of the ISS. These projects are connected (i) with tests of relativity (SUMO – PI J. Lipa, PHARAO – PI C. Salomon, PARCS – PI D. Sullivan) thus exploiting the condition of large velocity changes, (ii) with setting up better time standards (PHARAO, PARCS, RACE – PI K. Gibble) using the condition of free fall what increases the interaction time of atoms with external fields, (iii) with the detection of cosmic high energy particles and anti-matter (AMS – PI S. Ting, EUSO), and (iv) with the thermodynamics and dynamics of phase transitions (SUE – PI J. Lipa, BEST – PI G. Ahlers, MISTE – PI M. Barmatz, DYNAMX – PI R. Duncan, EXACT – PI M. Larson) in liquid helium (superfluid lambda transition and liquid-gas critical point) using an environment without any gravitational force at a level that would destroy the homogeneity of the sample.

### ***SUMO: Superconducting Microwave Oscillator Experiment***

**Scientific Objectives:** The Superconducting Microwave Oscillator experiment (SUMO) is designed to perform tests in special relativity, and in conjunction with PARCS (see below) a differential red-shift test of general relativity. Also, it will support PARCS by providing it with a low noise oscillator signal on short time scales. It will be located in the Low Temperature Microgravity Physics Facility (LTMPF) that will be attached to the Japanese Experimental Module JEM-EF close to PARCS and will be connected to it with a fiber-optic link.

Tests of special relativity typically fall into two main classes: one involving angle-dependent effects and the other absolute velocity effects. A model of potential Lorentz violations was developed by Mansouri and Sexl [15] who considered the possibility of

an anisotropic propagation velocity of light relative to a preferred frame. In this model if a laboratory is assumed to be moving at a velocity  $v$  at an angle  $\mathcal{G}$  relative to the axis of a preferred frame, the speed of light as a function of  $\mathcal{G}$  is given by

$$\frac{c(\mathcal{G}, v)}{c} = 1 + \left( \frac{1}{2} - \beta + \delta \right) \frac{v^2}{c^2} \sin^2 \mathcal{G} + (\beta - \alpha - 1) \frac{v^2}{c^2} \quad (0.6)$$

where  $\alpha$  is the time dilation parameter,  $\beta$  is the Lorentz contraction parameter, and  $\delta$  tests for transverse contraction, to be determined either experimentally or in the particular theory being considered (this is a special case of Eq.(0.1)). In Special Relativity the last two terms on the right hand side of Eq.(0.6) are zero. For an experiment on the ISS the velocity relative to inertial space would be modulated at orbital rate, giving rise to a periodically varying clock signal. It is well established [16] that the frequency of an atomic clock is independent of the velocity vector to very high precision. In the case of the  $\mathcal{G}$ -dependent term, a signal could be generated by mounting two cavities at right angles, since their frequencies are sensitive to the velocity of light only in the radial directions. At present the best limit [17] on this form of isotropy is  $(1/2 - \beta + \delta) < 2.2 \cdot 10^{-9}$ . By comparing the frequencies of two orthogonally mounted cavities at twice orbital rate, the limit for this effect could be improved of a factor of about 100 with 60 days of averaging. The present limit [18] on the  $\mathcal{G}$ -independent term is  $|\beta - \alpha - 1| < 6.9 \cdot 10^{-7}$ . With a frequency stability of  $5 \cdot 10^{-16}$  referencing to PARCS, and averaging over 4 months, we would expect to set a limit of  $\sim 6 \cdot 10^{-10}$ , a factor of  $\sim 10^3$  improvement. This signal would be modulated at orbital rate.

Recently Kostelecky and Mewes [19] have pointed out that in the general Standard Model Extension (SME) that permits weak Lorentz violations additional terms may exist which show signatures different from those expressed in Eq.(0.6). In particular, quantities independent of  $v$  and others linear in  $v$  may exist which could be detectable in certain types of experiment. A configuration of interest is a pair of cylindrical microwave cavity resonators operating on radial modes, one with its axis aligned in the direction of rotation and the other with its axis at  $45^\circ$  to the axis of rotation. In the most general case the beat signal  $\Delta\nu$  from such a pair is predicted to have terms of the form

$$\frac{\Delta\nu}{\nu} = A_S \sin(\omega t) + A_C \cos(\omega t) + B_S \sin(2\omega t) + B_C \cos(2\omega t) + const \quad (0.7)$$

where the coefficients are linear combinations of potential Lorentz violating terms and  $\omega$  is the rotation rate of the pair of cavities (this is another realization of (0.1)). The quantities  $A$  and  $B$  include the effects described by Eq.(0.6) at second order of  $v/c$  but also terms that probe for additional physics possibly due to residual effects left over from the birth of the universe. There are nineteen possible Lorentz-violating parameters contributing to  $A_S$ ,  $A_C$ ,  $B_S$  and  $B_C$ , of which ten are bounded by astrophysical data. SUMO is sensitive to seven linear combinations of the remaining nine parameters. Bounds at the  $10^{-17}$  level are expected for the velocity independent terms, and at the  $10^{-14}$  level for those proportional to  $v$ .

The LPI principle of general relativity states that the outcome of any non-gravitational experiment conducted in a local, free-falling frame is independent of where and when that experiment is conducted. A consequence is that different types of clocks keep exactly the same time, no matter where they are co-located in the universe, provided that the laws of physics do not vary from place to place. One of our goals is to look for a violation of LPI by comparing a microwave cavity frequency with that of an atomic

clock as a function of position and gravitational potential as the ISS orbits the earth and the sun. A microwave cavity and an atomic clock have different dependencies on fundamental physical constants [20] which may reveal a violation of LPI. Alternatively, one can view the experiment as setting limits on effects predicted by various theories competing with general relativity as descriptions of the interaction of matter and spacetime, or a search for new physical phenomena. This test could improve on the earlier measurement by a factor of about 1000. SUMO will require two to four months of operation in order to achieve its science objectives.

**Experimental Payload:** The SUMO experiments will be performed on board the ISS inside the LTMPF, a liquid helium cryostat allowing access to temperatures down to 1.4 K for up to several months. The central part of the payload consists of two cylindrical superconducting microwave cavities mounted with their axes orthogonal. A conceptual design of the SUMO instrument is shown in Fig.2. It consists of a vacuum flange which is attached to the helium tank of the LTMPF, a thermal isolation system, and a pair of microwave cavities.

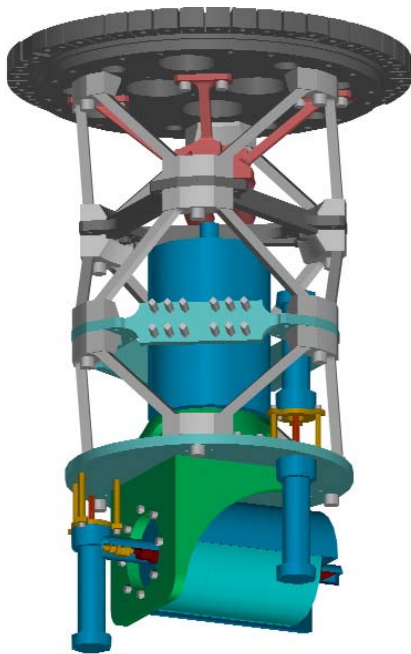


**Figure 2:** Conceptual view of SUMO instrument. The diameter of the structure is about 20 cm.

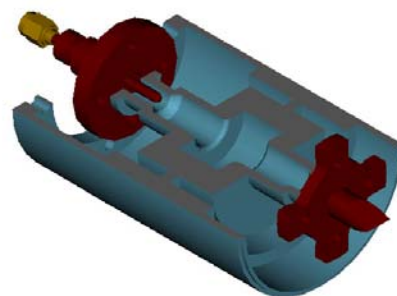


**Figure 3:** Cut-away view of a microwave cavity for the SUMO mission. Its radius is about 1.3 cm. Due to its special design this cavity is very robust against microgravity noise.

The cavity design includes a special mounting structure which reduces its acceleration sensitivity by a factor of  $\sim 1000$ . This was necessary to reduce the effect of residual drag on the ISS which has a component at the orbital period. A cut-away view is shown in Fig.3. The cavity is in the central section and is supported symmetrically by the outer structure that is bolted to the thermal isolation system at one end. The multi-stage thermal isolation system is designed to allow temperature control in the  $10^{-9}$ K range using specially designed paramagnetic thermometers with extremely low noise.

**Mission Scenario:** The ISS has a low Earth circular orbit with a height of approximately 350 km, and an inclination of approximately  $50^\circ$ . Therefore the velocity

change of the apparatus during one orbit is about a factor of fifteen larger than that available on the Earth's surface (the orbital period of the ISS is just over 1.5 h). While the gravitational potential differences are typically rather small, they can be enhanced by flying in a slightly elliptical orbit. Typically the ellipticity is  $\sim 0.002$ , while values of 0.003 are allowed under normal flight rules. SUMO will be requesting the highest possible ellipticity to enhance the driving term for any red-shift violation. The expected cyclical changes are significantly larger than those available on the ground on short time scales. By making use of the ISS orbital position information it will be an easy matter to keep track of the changing gravitational potential for correlation with the SUMO/PARCS difference signal. Also, by varying the location of the orbital nodes during the mission, it will be possible to separate any signal from that caused by a Lorentz violation which would be fixed in inertial space. Estimates of the ISS vibrational noise in all frequency ranges indicate it should not be a serious problem using the low acceleration sensitivity cavities.

### ***ACES/PHARAO: Atomic Clock Ensemble in Space/Projet d'Horloge Atomique par Refroidissement d'Atomes en Orbite***

**Scientific Objectives:** This mission [21] intends (i) to set up the PHARAO clock on the International Space Station, and to study its performance in space. (ii) Together with a hydrogen maser, to establish a time scale which can be compared with terrestrial clocks to an accuracy of  $10^{-16}$ —which would be an enormous improvement over the present level of synchronization that is possible using GPS (Global Positioning System) clocks. Thus an ultra-high performance global time-synchronization system should be realised, which will make possible new navigation and positioning applications. (iii) To perform tests of the Gravitational Red Shift (with an improvement of more than a factor ten over present tests) and to search for a time-dependence of the fine structure constant  $\alpha$  to a relative precision level of  $10^{-16}$  per year. This will be accomplished by comparison between the ACES clocks and ground clocks of various types such as rubidium fountains and optical clocks. (iv) To search for an anisotropy of speed of light by analysing the propagation of microwaves in different directions when ACES clocks are compared with ground clocks.

**Experimental Payload:** the payload consists of the PHARAO clock, based on a fountain of cold Cesium atoms, and hydrogen-maser clock. Additional components are the MWL (MicroWave Link), replacing the formerly considered optical communication link T2L2 (Time Transfer by Laser Link), which was to send short bursts of light (100 picoseconds) between clocks on Earth and the clocks on the ISS, to synchronize them. The payload will be placed on an external platform of the European module columbus in a nadir position.

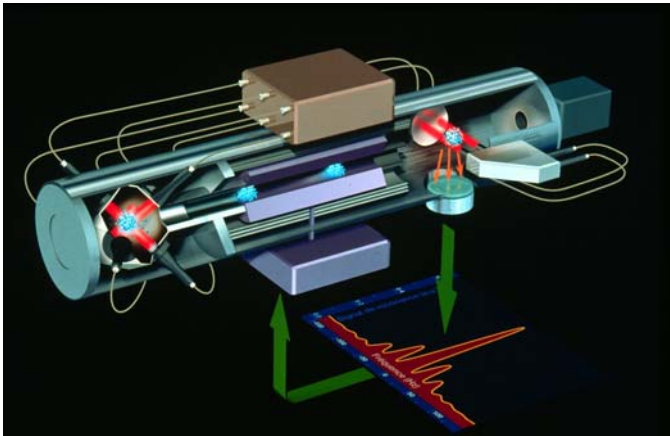


**Figure 4:** Principle of PHARAO , a cold atom clock in microgravity. An optical bench (top) provides light to a cesium tube for cooling and detecting the atoms using optical fibers. Atoms are collected in optical molasses in a first chamber (left), cooled below  $1 \mu\text{K}$  and launched into a second chamber. They enter a cavity in which they experience the two suc-



cessive Ramsey interactions with a microwave field tuned near the 9.192 631 770 Hz cesium frequency. Atoms excited by this field are detected downstream by fluorescence. The resonance signal is used to lock the oscillator's central frequency to the cesium transition. For a launch velocity of 5 cm/s, the expected resonance width is 0.1 Hz, ten times narrower than in Earth fountains.

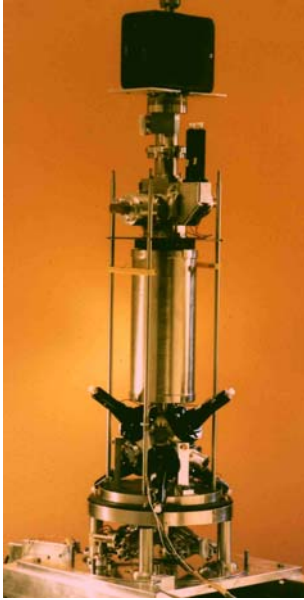


**Figure 5:** The zero-g qualified prototype of an atomic clock for space: the cooling zone is at the bottom, the interaction zone in the middle, and the detection zone at the top. The length of the apparatus is approximately 1 metre.

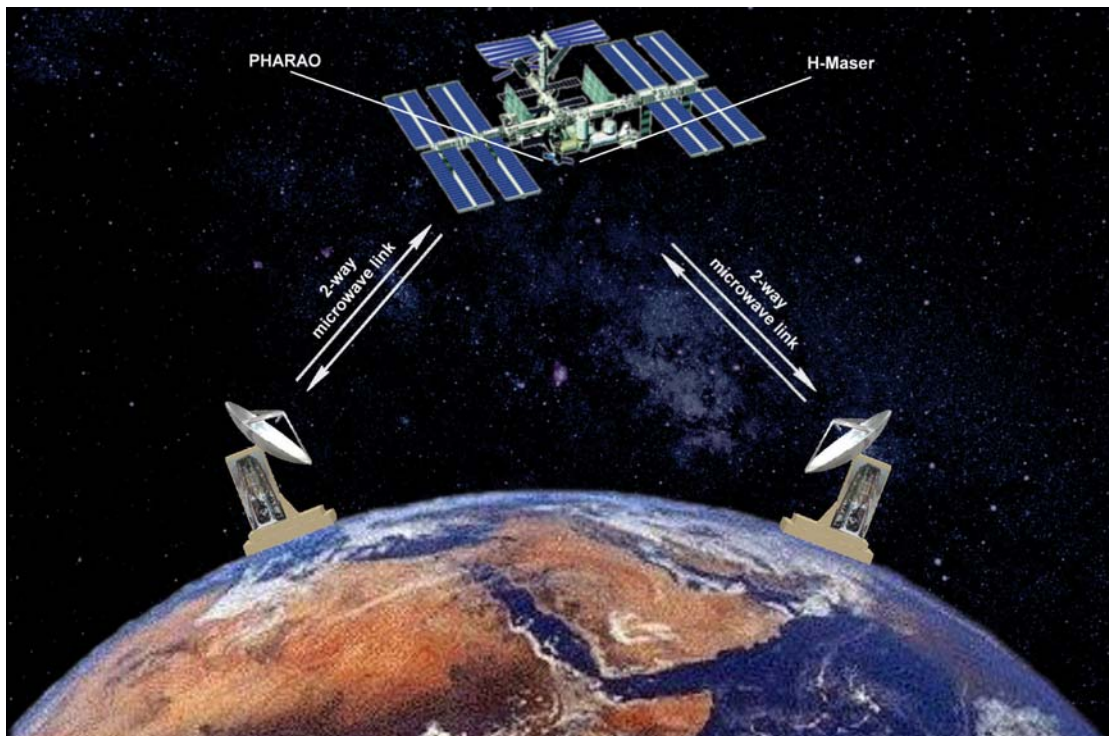


**Figure 6:** The ACES ensemble consisting of the PHARAO clock, and the hydrogen maser clock. Optical and microwave links establish connections to Earth for time and frequency transfer.

**Mission Scenario:** The MWL will operate by sending signals from Earth to the ISS where the arrival time will be recorded, and where the signal will also be back to Earth. From the signal's 'round trip' it will be possible to eliminate any fluctuations in the travel time due to the atmosphere. The mission is planned to run for 18 months.

**Technology:** In this mission—for the first time—laser cooling techniques and atom traps will be established and tested in space. Furthermore, also for the first time the performance of atom-optical elements can be tested in space. All these techniques will be of importance for future satellite missions. In addition, appropriate microwave links will be developed.

**Further information:** <http://opdaf1.obspm.fr/www/pharao.html> ,  
<http://www.cnes.fr/activites/connaissance/physique/lindex.htm>

### *PARCS: Primary Atomic Reference Clock in Space*

**Scientific Objectives:** PARCS is an atomic-clock mission scheduled to fly on the International Space Station (ISS) in 2008. The mission, funded by NASA, and being a collaboration between JPL, NIST and the University of Colorado, involves a laser-cooled cesium atomic clock, and a time-transfer system using a Global Positioning System (GPS) receiver within the instrument to provide position, velocity, and timing information. PARCS will fly concurrently with SUMO (Superconducting Microwave Oscillator). SUMO will function as a stable local oscillator as well as a clock with structure dependent on totally different physical phenomena. The objectives of the mission are to:

- Test gravitational theory by measuring the gravitational redshift and performing other measurements which probe the foundations of the Special and General Theories of Relativity;
- Study laser-cooled atoms in microgravity;
- Improve the accuracy of timekeeping on earth.

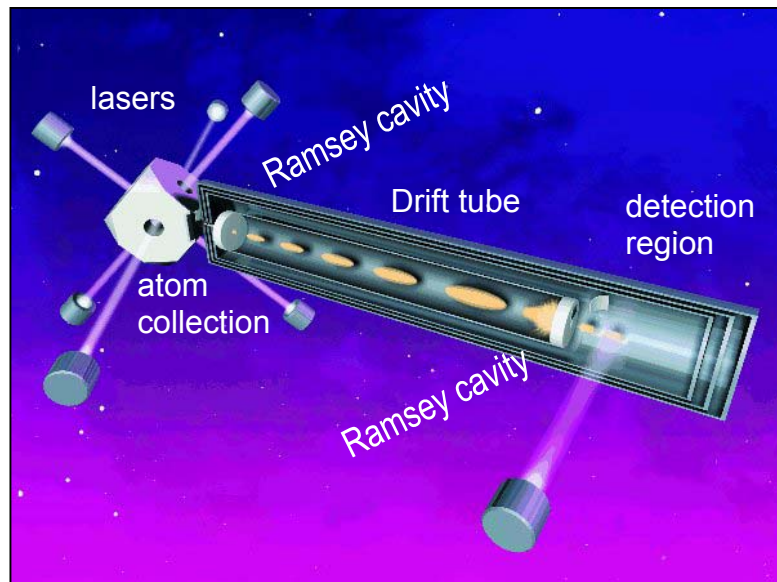


**Figure 7:** Schematic view of the PARCS clock, showing the laser-cooled atom collection region, Ramsey cavities, drift tube, and detection region.

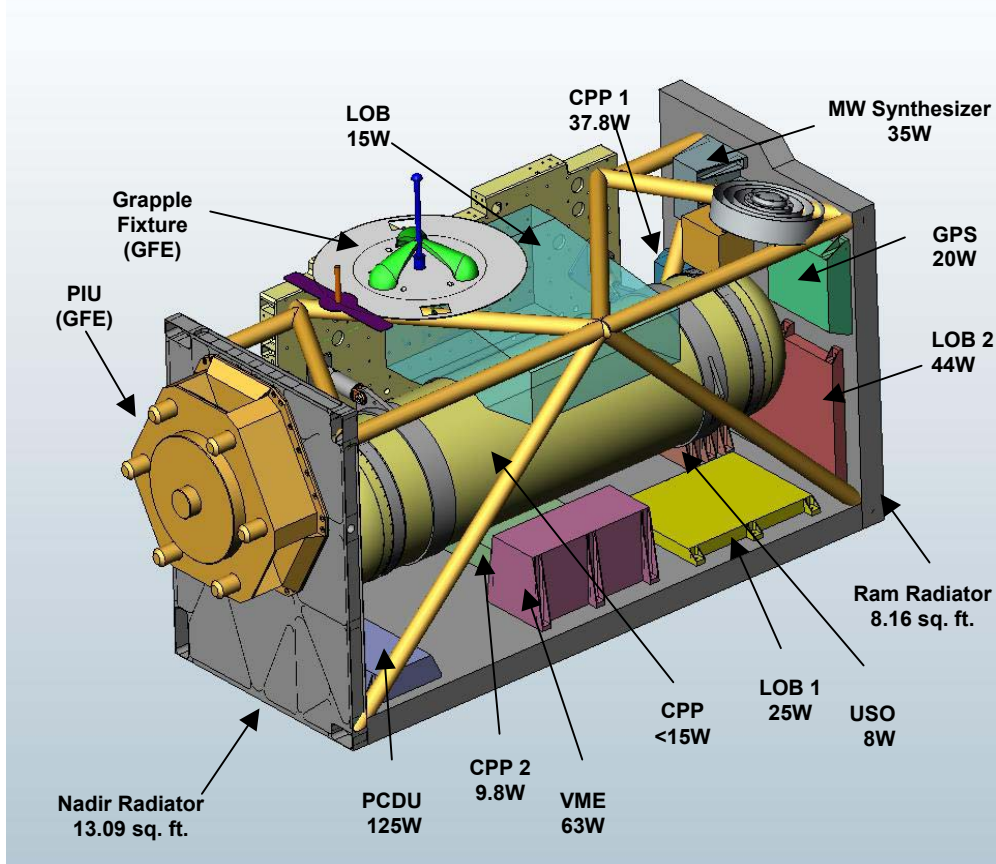


**Figure 8:** The major subsystems of PARCS consists of (i) a Laser Optical Bench (LOB), (ii) a Cs Physics Package (CPP), (iii) a Microwave Synthesizer, (iv) a GPS Receiver, (v) Avionics, (vi) Instrument Electronics, and (vii) Structure/Thermal Control.

**Technology and Mission scenario:** The proposed ISS location for the experiment is on the External Facility of the Japanese Experimental Module (JEM). This location affords a good view of the GPS satellite constellation, needed for comparing space and ground clocks. In addition, the available volume, power, and cooling system on the JEM are well matched to mission requirements.

The microgravity environment of space affords the possibility of slowing atoms down to speeds well below those used in terrestrial atomic clocks, allowing for substantial improvement in clock accuracy and stability. Clock stability of  $7 \times 10^{-14}$  at one second, and accuracy better than  $10^{-16}$ , are projected. The GPS measurement system will provide continuous position information to within 10 cm, and velocity measurements better than 0.13 mm/s. The frequency shift of the orbiting clock can be compared to reference clocks on earth with uncertainties expected to be less than 2 parts

per million, and relativistic corrections to be applied to the orbiting clock so that it can serve as a truly international time standard available worldwide. PARCS will be compared continuously to the SUMO oscillator, allowing improvements in tests of relativity such as in the Kennedy-Thorndike and Michelson-Morley experiments, and in tests of local position invariance. The following table summarizes the goals of the PARCS mission.

Table 1. Summary of science objectives for PARCS

Measurement/Test	Expected Uncertainty	Previous Best Uncertainty	Improvement (Ratio)
Net Frequency Shift, $\Delta f / f$	$1.7 \times 10^{-6}$	$70 \times 10^{-6}$	35
Gravitational Frequency Shift, $\Delta f / f$	$12 \times 10^{-6}$	$140 \times 10^{-6}$	12
Kennedy-Thorndike, $\beta - \alpha - 1$	$9 \times 10^{-10}$	$6.0 \times 10^{-7}$ [18]	770
Local Position Invariance, $\alpha_{AB}$	$9 \times 10^{-6}$	$2.1 \times 10^{-5}$ [21]	2.3
Michelson-Morley, $1/2 - \beta + \delta$	$5 \times 10^{-10}$	$2.2 \times 10^{-9}$ [17]	5
Atom Drift Time, value in seconds	10	1	10
Accuracy of Space Clock, $\Delta f / f$	$5 \times 10^{-17}$	$1 \times 10^{-12}$	20,000
Realization of the Second, $\Delta f / f$	$5 \times 10^{-17}$	$1 \times 10^{-15}$	20

**Further information:** [www.boulder.nist.gov/timefreq/cesium/parcs.htm](http://www.boulder.nist.gov/timefreq/cesium/parcs.htm)

### ***RACE: Rubidium Atomic Clock Experiment***

RACE, the Rubidium Atomic Clock Experiment, is one of the three clock experiments planned for the ISS. RACE will be based on Rubidium atoms instead of Cesium. At laser-cooling temperatures, quantum mechanical effects dominate in atomic collisions. This leads to potentially very large cross sections and these collisions can produce very large frequency shifts in laser-cooled clocks [22] as shown in Figure 9. The collision shift is the largest systematic error in Cs fountain clocks. By using Rb, RACE avoids this large error source since, for  $^{87}\text{Rb}$ , the shift is much smaller than that for Cs [23,24].

**Scientific Objectives:** We have three primary goals for RACE: (1) Demonstrate new clock techniques for laser-cooled atoms to enable frequency comparisons with accuracies of 1 part in  $10^{17}$ . (2) Significantly improve the classic clock tests of general relativity. (3) Distribute accurate time and frequency from the ISS. RACE is currently scheduled to fly on the ISS in 2010. We review the design constraints and discuss the schematic for RACE.

The tremendous advantage of microgravity for atomic clocks is much longer interrogation times and hence very narrow transition linewidths. A microgravity design has some very different design constraints than earth-based fountain clocks. Essential to achieving high accuracy with RACE is a high short-term stability. To achieve the high stability, atoms must be

multiply launched – that is using the long interrogation time that microgravity provides (e.g. 10s) while launching atoms at a high rate (5 balls per second).

**Technology:** RACE will use a double-MOT<sup>i</sup> design to multiply launch atoms. This design allows a high throughput of cold atoms and therefore a high short-term stability. The high throughput is possible as the double-MOT can rapidly capture many cold atoms and then efficiently launch them through a clock cavity. The “upper” vapor cell trap in Fig.10 essentially continually traps atoms and then launches them at 5-10 m/s to the UHV trap “below.” Because of the high launch velocity from the vapor cell trap, the atoms pass quickly through the shutter separating the 2 traps. This implies that the shutter only needs to open for the short time the ball of atoms flies through and, only during that time, the lasers for the vapor-cell trap must be extinguished (so that no laser light enters the interrogation region). The real advantage of the double-MOT design is that the UHV trap can capture and launch a ball of atoms in as little as 5 ms [25]. This implies that the shutter separating the UHV trap and interrogation region only has to close for 5 ms for each launch and therefore is nearly always open. This allows a high through-

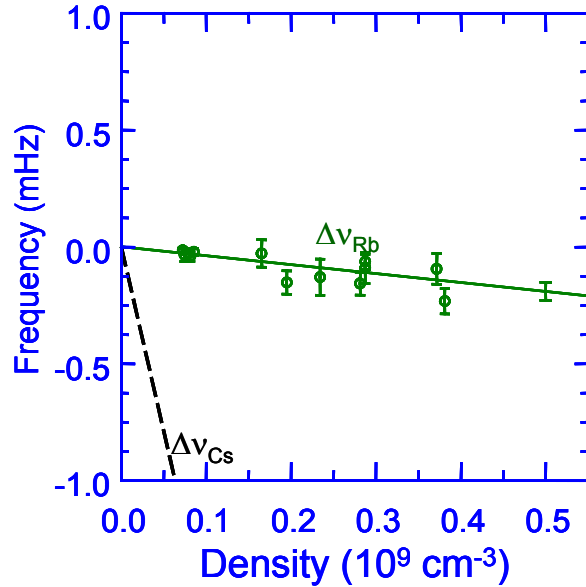


**Figure 9:** The measured collision shift for clocks based on cold Rb and Cs atoms. The shift for  $^{87}\text{Rb}$  is 50 times smaller than that for Cs.

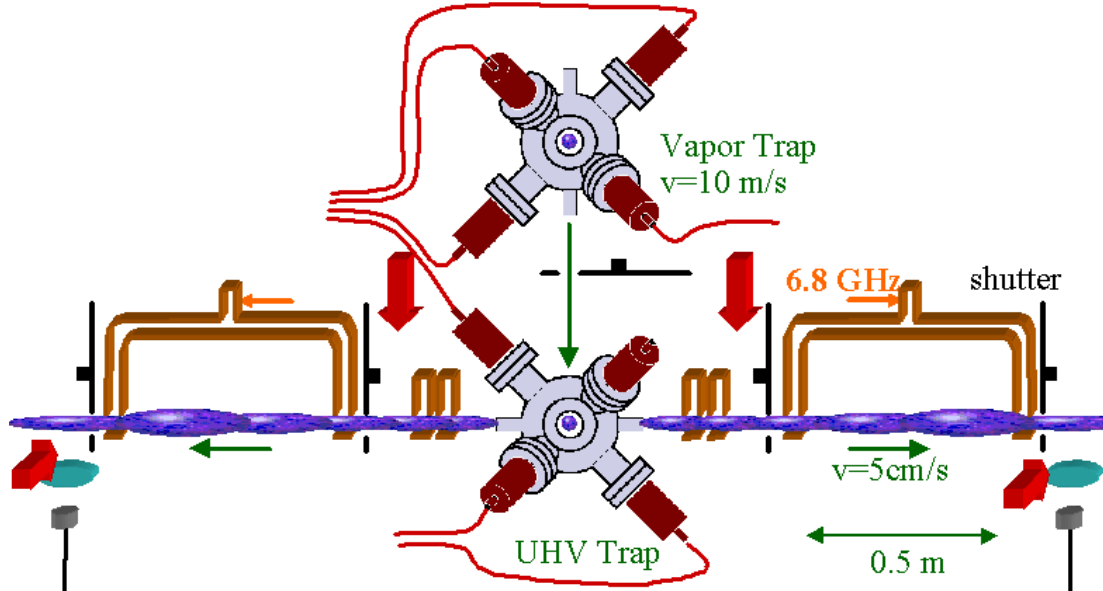


**Figure 10:** Schematic for juggling microgravity Rb clock RACE. Atoms are collected in the Vapor Trap and tossed to the UHV trap with a large velocity. The UHV trap captures the cold atoms and tosses them left or right to go through one clock cavity or the other.

put since the ball of atoms will have expanded considerably before reaching the shutter.

The RACE schematic in Fig.10 shows two clock cavities. After atoms are collected in the “UHV Trap,” they are launched either to the left or right, through one cavity or the other.

Having two cavities is important for a number of reasons. One advantage is that it greatly reduces the requirements for the local oscillator. Few oscillators can perform at  $\sigma_y(\tau) = 3 \times 10^{-15} \tau^{-1/2}$  and there is significant work required to develop their flight worthiness. The essential problem with only a single cavity is that the microwave frequency fed to the cavity must be switched from one side of the transition line to the other. During the switchover, the atoms must be cleared from the cavity and this means the oscillator is not tracked for some time. With 2 cavities, we can perform the switchover for one cavity while still monitoring the oscillator with the other cavity and therefore the stability of the clock is not compromised by the local oscillator's instability. Other advantages include eliminating the vibrational noise of the ISS, an independent check on the AC Start Shift due to blackbody radiation, and instrument redundancy.

Criteria	Goal
Short-term clock stability	$3 \times 10^{-15} \tau^{-1/2}$
Clock Accuracy	$1 \times 10^{-17}$
Gravitational Red Shift	$2.4 \times 10^{-7}$
Second-order Doppler	$3 \times 10^{-8}$
Kennedy-Thorndike ( $\beta - \alpha - 1$ )	$4 \times 10^{-11}$

Table 2. Mission performance goals for RACE. An improved Kennedy-Thorndike test requires the (re)flight of SUMO.

Performance goals for RACE are shown in Table 2. Flight with SUMO will allow high stability frequency comparisons for additional tests of fundamental physics.

### ***AMS: Alpha Magnetic Spectrometer***

The Alpha Magnetic Spectrometer AMS will place a sensitive particle detector in Earth orbit to learn the makeup of the particles that exist in the cosmic void. The detector will enable the determination of the number, energy, and charge of the particles that bombard the Earth from space. This information will then be used to determine how much antimatter exists in space, and, by extension, how much matter and of what type exists in the Universe. AMS is therefore a major cosmology experiment, and it will be capable of observing the properties of electrons, positrons, protons, antiprotons, and nuclei in high-energy 'cosmic' radiation from space. These observations may answer important questions about the Big Bang, including "Why did the Big Bang make so little antimatter?" and "What makes up the Universe's invisible mass?"

Because charged particles such as antiprotons are absorbed by the Earth's atmosphere (through collisions with protons, for example), the Alpha Magnetic Spectrometer must be taken up above the atmosphere into space, so that it can make effective measurements of these particles. The AMS experiment will therefore be placed on the International Space Station, where it will be left for several years to accumulate readings. A predecessor of AMS, the 1998 AMS experiment, was taken up into space by the Space Shuttle, and was the first sensitive particle detector to be placed in orbit. This early experiment was particularly helpful in calibrating the instrument, so that a future mission will be able to take even more accurate measurements. As the fundamental laws that govern our Universe are scrutinised ever more closely, such basic

questions as ‘what are the ultimate building blocks of matter?’ or ‘what are the fundamental forces through which these basic particles interact?’ are being asked. AMS will take a step toward answering these most fundamental questions.

**Mission Scenario:** The AMS detector will be placed on the ISS main truss, making full use of the ISS’s irreplaceable support systems, and will gather particle data for 3 years.

**Technology:** A transition radiation detector will give the velocities of the highest energy particles, whilst a silicon tracker will follow the particle paths through the instrument. A very significant weight- and volume-saving has been made in the design of the apparatus by using a superconducting magnet to produce the very high magnetic field of AMS. The magnet, wound with persistent supercurrent-carrying Nb/Ti wire will operate at a temperature of 1.8 K, cooled by 360 kg of superfluid liquid helium. The curvature of particle paths through such a magnetic field will give the momentum/charge ratio for each detected particle, plus the all-important sign of the charge. In addition, AMS will employ particle time-of-flight counters, a ring-imaging Cherenkov radiation detector, an electromagnetic calorimeter, and an anti-coincidence counter to veto any spurious particles that may pass sideways through the apparatus.

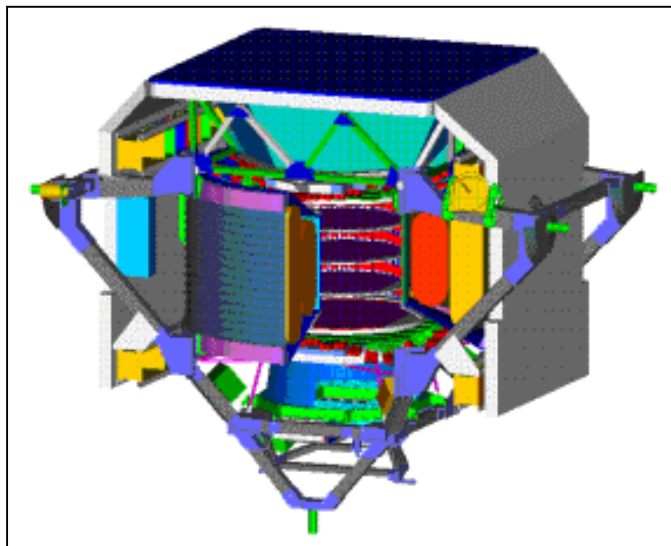


Figure 11:

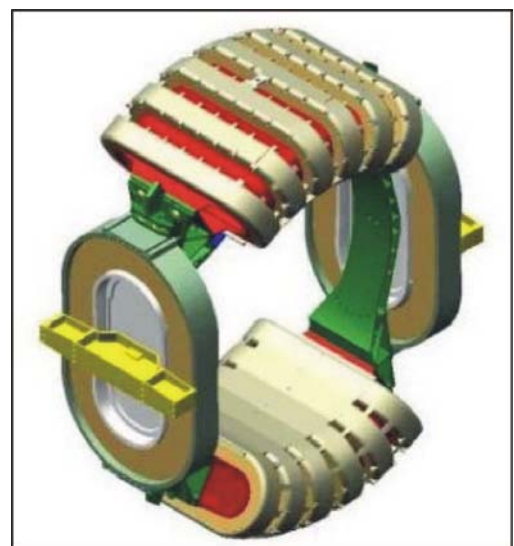


Figure 12: The AMS magnet consists of 14 superconducting coils arranged to give a dipole field with minimal external stray field.

**Further information:**

<http://spaceflight.nasa.gov/shuttle/archives/sts-91/orbit/payloads/ams.htm>,  
<http://ams.cern.ch/AMS/Description/overview.html>.

### ***EUSO: Extreme Universe Space Observatory***

**Scientific background:** One of the most challenging issues in Astroparticle Physics is represented by the detection and observation of EECRs (Extreme Energy Cosmic Rays): the existence of sub-atomic particles with individual energies above 10 J (the

kinetic energy of a tennis ball launched by an expert player, but concentrated in a single proton or neutrino !) raises fundamental scientific questions about their origin and propagation in the interstellar and intergalactic space (for various reviews see [26]). The Earth's atmosphere constitutes the ideal detector for the EECRs and the companion Cosmic Neutrinos. These EECR particles, interacting with the atmosphere, give rise to propagating Extensive Air Showers (EAS) accompanied by isotropic emission of UltraViolet (UV) fluorescence (300-400 nm wavelength range). These are induced in the Nitrogen of the atmosphere by the secondary charged particles in the EAS, as result of a complex relativistic cascade process; an isotropically diffuse optical-UV signal is emitted following the impact of the Cherenkov beam, accompanying the EAS, on clouds, land or sea. An EAS corresponding to a primary particle with energy  $E > 10^{19}$  eV forms a significant streak of fluorescence light over 10-100 km along its passage in the atmosphere, depending on the nature of the primary, and on the pitch angle with the vertical. The extremely low value for the EECR flux, corresponding to about 1 event /km<sup>2</sup> per century at  $E > 10^{20}$  eV, and the extremely low value for the interaction cross section of neutrinos, make these components difficult to observe. The solution is to employ a detector with high values for the effective area and target mass.

The highest energy event ever measured was observed by the Fly's Eye experiment, at  $3 \times 10^{20}$  eV, or about 50 J; the Fly's Eye experiment was a fluorescence detector, a forerunner of the presently operating HiRes experiment. The shower evolution of this specific event is quite consistent with the particle being a proton, the simplest possible explanation. At such energies particles such as protons cannot no longer be confined by the magnetic field of our Galaxy, and so these events almost certainly come from outside our Galaxy. In fact there are few astronomical sites known which could even confine particles at such energies; the Larmor radius has to fit inside the source region for any acceleration process to work at all; also since even protons at such energies have appreciable losses in photon interaction and also by synchrotron losses in magnetic fields, those losses must be balanced by any acceleration process. One solution for this conundrum is weakly relativistic shock waves in radio galaxy hotspots. Another solution to the acceleration problem is to suggest that these particles are the result of the decay of an even heavier postulated particle, such as a topological defect originally formed in the Big Bang. In that picture there is no problem with any acceleration site; this process could happen anywhere. In either picture the resulting particles must still traverse the photon field of the Big bang, which induces a general cut-off – the so-called GZK-cut-off<sup>2</sup> at  $5 \cdot 10^{19}$  eV ; this cutoff should exist for a homogeneous source distribution, no magnetic field effects at all, and a source spectrum which goes to much higher energies of the protons (other known particles give similar, usually lower cutoff energies). In the acceleration picture this means that we have to find a source, better many possible sources, and in the decay model we have to identify a long-lived particle that exists as a residual from the Big bang in sufficiently large number density and lifetime to work as a candidate source particle.

---

<sup>2</sup> The GZK-cut-off, named after the three physicists K. Greisen, G.T. Zatsepin, and V.A. Kuzmin is the effect that high energy particles interact with the photons of the cosmic microwave background and create massive particles. As a consequence, particles with an energy of  $10^{20}$  eV upon arrival at Earth cannot come from a distance larger than 100. A possible solution of this puzzle is the hypothesis of a violation of Lorentz invariance at high energies [27,3].



So, either of these two main very different concepts have major problems: In the notion that we have a cosmic source, which specifically accelerates protons to very high energy, we find at best one source at the top particle energy, and that is the radiogalaxy M87; at lower energy there are many sources. However, in order to obtain the near isotropy of the events on the sky in their arrival direction distribution, we either need many sources or a near complete scrambling of directions by magnetic fields, either in our cosmic neighbourhood, or in the Galactic halo. Both is possible, but completely unproven. In the other main picture, that these events derive from the decay of a new unknown particle, we face equally difficult choices: We have to invent such particles, whose existence is plausible, but they have to have an extremely long lifetime to survive through to today from the Big Bang, and yet decay locally in just the right numbers to give that flux observed. These leads to just as great a problem as the first major approach.

In either concept we can expect to learn new physics: In the notion that the particles are accelerated, perhaps in radio galaxy hot spots, then in some such radio galaxies, the particles would mainly interact in the source, and we could perhaps observe the long lived decay products of the particles produced in these interactions. In the decay concept, we might expect that there is a connection to the dark matter particles which are generally accepted to make up the bulk of all galaxy masses. Maybe it is the dark matter particles themselves that decay.

Last, there should be some connection to the very energetic gamma ray flashes or Gamma Ray Bursts (GRBs): Since these GRBs seem to occur in some fraction of all supernova explosions, there should be one that was last in our Galaxy, or other nearby well studied galaxies, and that might be observable in its residual signal. After all, supernova explosions are accepted to produce most, if not all Galactic cosmic rays, up to energies of  $3 \times 10^{18}$  eV. In those special cases, where GRBs accompany the supernova explosion, higher particle energies might be reached. Again, new physics will be learnt, then in some local well studied neighbourhood.

These are just some well established examples of concepts that may explain the occurrence of high energy particles, and all can be expected to teach us new physics, far beyond any that Earth-bound accelerators can give, but still below what the Big Bang itself involves, so with the ultra high energy cosmic ray particles, we may expect to go beyond today's world in physics, to then reach the ultimate energy of the Big Bang and then the fundamental scale where all forces of Nature combine.

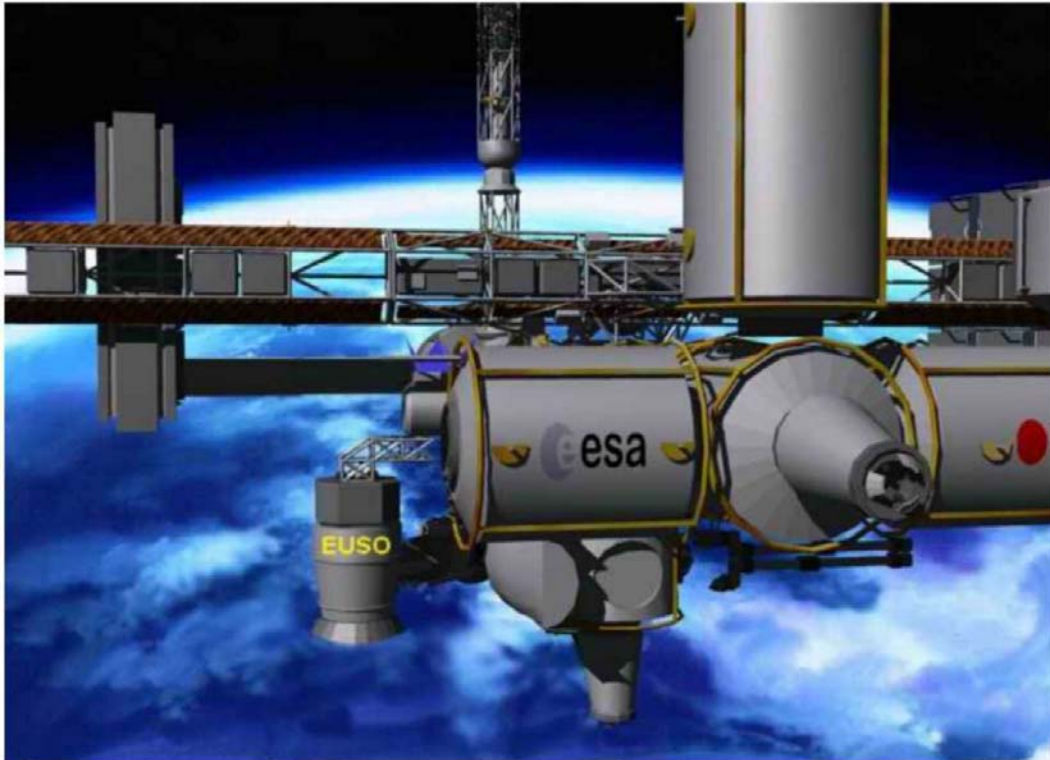


**Figure 13:** EUSO ist placed externally to the European Columbus module.

**The mission:** The “Extreme Universe Space Observatory – EUSO” is the first Space mission devoted to the investigation of cosmic rays and neutrinos of extreme energy ( $>5 \times 10^{19}$  eV), using the Earth’s atmosphere as a giant detector. The detection will be performed by looking at the streak of fluorescence light produced when such a particle interacts with the Earth’s atmosphere. EUSO will observe the fluorescence signal looking downward from Space into the dark Earth’s atmosphere, over a  $60^\circ$  full field-of-view. Fluorescence light will be imaged by a large Fresnel lens based optical system onto a finely-segmented focal surface detector. The highly focal surface segmentation and the fast time resolution of the detector will allow reconstruction of the shower’s arrival direction and energy with high precision. EUSO is expected to detect of the order of one thousand EECRs per year with  $E > 10^{20}$  eV, and to open a window into the High Energy Neutrino Universe. EUSO is a mission of the European Space Agency ESA, with a goal for a three year mission starting in 2009. EUSO will be accommodated, as an external payload of the Columbus module, on the ISS (Fig. 13).

The integrated exposure (about  $2 \times 10^3$  km<sup>2</sup> yr sr) available today for the ground based arrays over the world is sufficient only to show the existence of the “ankle” feature at about  $5 \times 10^{18}$  eV in the Cosmic Ray energy spectrum. With the current total exposure, the subset of available data is of only about twenty events in total exceeding  $10^{20}$  eV; the limited statistics of the available data excludes the possibility of observing significant structures in the energy spectrum at higher energies. Experiments carried out by means of the new generation of ground based observatories, HiRes (fluorescence) and Auger (hybrid), will still be limited by practical difficulties connected to a relatively small collecting area ( $< 10^4$  km<sup>2</sup> sr) and by a modest target mass value for neutrino detection.

Early in the eighties, J. Linsley, who was also the first to claim detection of a  $10^{20}$  eV event, suggested that a solution can be provided by observing from space, and at night, the UV fluorescence induced in the atmosphere by the incoming extraterrestrial radiation; this potentially will enable the exploitation of up to millions  $\text{km}^2 \text{sr}$  for the acceptance area, and up to  $10^{13}$  tons of atmosphere as the target for neutrino interaction. This is the philosophy of the “AirWatch Programme”, and EUSO is the first space mission developed within the AirWatch framework.

When viewed continuously, a target object for EUSO moves on a straight path with the speed of light. The resulting picture of the event seen by the detector looks like a narrow track in which the recorded amount of light is proportional to the shower size at the various penetration depths in the atmosphere. From a Low Earth Orbit space platform the UV fluorescence induced in atmospheric nitrogen by the incoming radiation will be detected by EUSO, and studied. Other phenomena such as meteors, space debris, lightning, atmospheric flashes, can also be observed by EUSO; on the other hand the luminescence coming from the EAS produced by the Cosmic Ray quanta can be disentangled from the general background and measured, by exploiting its fast-timing characteristic feature.

**Further information:** <http://www.euso-mission.org/>

### ***SUE: Superfluid Universality Experiment***

The Superfluid Universality Experiment (SUE) is a developmental program that ultimately may fly in the LTMPF. It is concerned with the study of the second order phase transition that occurs when helium is supercooled into a liquid, and further cooled into a superfluid, in a microgravity environment under a range of different pressures. Due to fundamental theoretical difficulties there exists no exact treatment of these transitions, limiting our ability to perform decisive tests of the theory. However, the theory [4] makes some exact predictions concerning the exponents which characterise the singular behaviour of many properties near the transition. Of prime importance is the prediction of 'universality', which states that the exponents have the same value for wide classes of systems independent of the strength of the microscopic interaction or of certain macroscopic thermodynamic parameters. For example, in liquid helium just below the superfluid transition temperature,  $T_\lambda$ , the exponent  $\zeta$  of the superfluid density,  $\rho_s = \rho_o(P) t^\zeta$ , is predicted to be a universal constant close to  $2/3$ , where  $t = 1 - T/T_\lambda(P)$  is a dimensionless parameter measuring the temperature distance from the transition. In contrast, the amplitude,  $\rho_o(P)$ , is predicted to be a non-universal quantity depending on the isobaric pressure,  $P$ , at which  $\rho_s(t)$  is measured. The superfluid density, which is not directly measurable, can be related to the velocity of second sound and the heat capacity through a thermodynamic argument. SUE will measure the velocity of second sound and the heat capacity along various isobars near the lambda line of helium, and from this determine the value of  $\zeta$  as a function of pressure. This information will directly test the universality hypothesis and any detected pressure dependence would nullify the theory. This test would be the most accurate performed to date on any phase transition, about a factor of 30 improvement on previous work [28]. The experiment needs to be performed in space to reduce the spurious effect of hydrostatic pressure on the measurements.

**Experimental Payload:** The core of the flight apparatus will consist of a thermally insulating cylindrical sample chamber about 3 cm long and 1 cm in diameter, filled with high-purity liquid helium. Attached to the sample chamber will be a thermom-

eter with a resolution of  $10^{-10}$  K and a superconducting pressure gauge. The sample chamber will form a second sound resonator and will be equipped with a detector having an extremely high sensitivity and with a second sound generator. The generator will be a thin film heater which will also be used to perform heat capacity measurements. This assembly will be placed within a multistage thermal enclosure functionally similar to that shown in the SUMO section above, and sketched below in Fig.14. The superconducting pressure gauge will be used as part of a constant pressure servo. A second, lower resolution absolute pressure gauge will also be attached to the cell. This will be used to establish the link to the ground-based second sound and heat capacity measurements and to calibrate the high resolution gauge. The walls of the vacuum enclosure will be maintained near 1.4 K to allow operation of the sample chamber at various temperatures along the lambda line. This basic operating temperature will be maintained by using the LTMPF cryostat, with an experiment time of 50 days needed for completing the measurements.

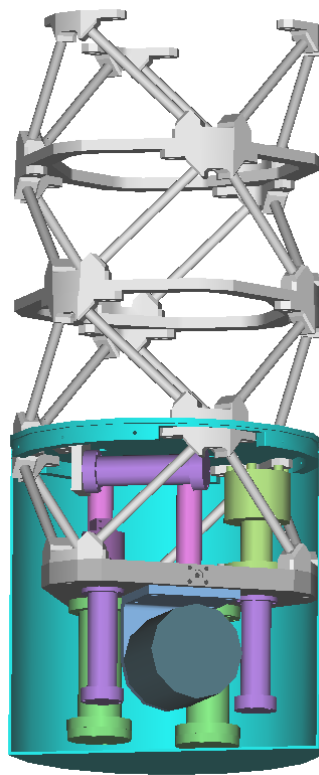


**Figure 14:** Schematic view of SUE instrument and thermal isolation structure.

**Mission Scenario:** The experiment will be located within the LTMPF and placed on the JEM-EF attached to the ISS. To perform the experiment, the density is first set at the desired value by adjusting the quantity of helium within the cell while referencing the absolute pressure gauge. Once the density is set, the pressure is controlled using the high resolution gauge and a flexible diaphragm. Next, the temperature of the cell is raised incrementally closer to the lambda point and the fundamental resonant frequency of the cavity is measured. Values in the range 0.25 to 500 Hz are expected. The heat capacity would also be measured at each temperature. The frequency, pressure, heat capacity and temperature measurements will be continued until the transition is reached, marked by the rapid decrease of resonant frequency and ultimate loss of signal. A number of temperature sweeps at a given density will be performed to

check for errors in the data and to estimate the uncertainties in the results near the transition. The density will then be reset and the measurement sequence repeated. A minimum of five different isobars will be explored, over the range 0-30 bar.

**Further information:** <http://chex.stanford.edu/sue/> ,  
<http://funphysics.jpl.nasa.gov/technical/ltcmp/sue.html>.

### ***BEST: Boundary Effects near Superfluid Transitions***

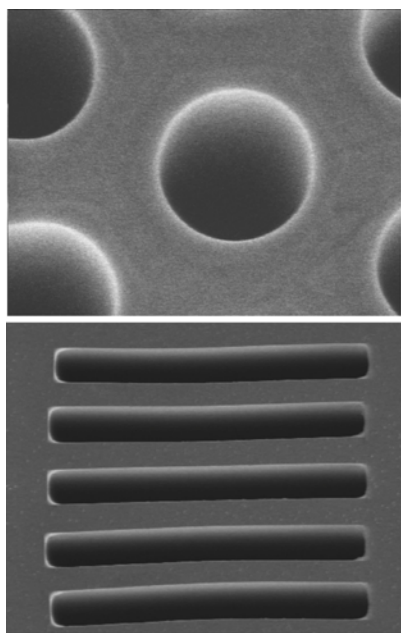


**Figure 15:** Scanning electron micro-graphs of micro-channel plates. Top:  $1\ \mu\text{m}$  diameter cylindrical pores. Bottom:  $5\ \mu\text{m} \times 50\ \mu\text{m}$  rectangular channels. In both cases, the holes can have a length (in the direction perpendicular to the page) of 1 to 5 mm. These micro-channel plates serve as the confinement medium of liquid helium. The hole diameter and channel dimensions can be varied from about  $1\ \mu\text{m}$  (as shown here) to about  $100\ \mu\text{m}$ .

**Scientific Objectives:** the study of molecular-level boundary issues, using liquid helium during phase transitions between the fluid and superfluid states in a microgravity environment. In detail, BEST will (i) improve the measurement of the thermal conductivity in a three-dimensional  $^4\text{He}$  sample along the lambda line, by three orders of magnitude, (ii) measure the thermal conductivity of  $^4\text{He}$  in one- and two-dimensional confinements of various sizes, and (iii) examine the cross-over behaviour from three-dimensional superfluid transitions to the fundamentally different two-dimensional superfluid transitions.

**Experimental Payload:** BEST intends to make use of the Low Temperature Microgravity Physics Facility (LTMPF, a large helium dewar) facility aboard the ISS. Superfluid Helium under various boundary conditions given by e.g. microchannel plates (see Fig.15) will be studied, using very sensitive thermometers, together with high precision pressure regulators.

**Mission Scenario:** It is planned that this experiment will be carried out over a period of 6 to 14 weeks aboard the ISS, which is sufficient time for the helium phase-transition to be studied along a number of different isobars, i.e. under a number of different hydrostatic pressures. In this way it should be possible to find out if the scaling-function for the lambda transition is universal—in the sense that it is pressure-independent. It is noteworthy that such an extended experimental campaign would not be possible aboard the space shuttle.

**Technology:** In order to explore such highly constrained helium samples, small high-resolution (nK) thermometers must be employed, along with high-precision pressure-regulators; and in order to perform the tests on the one- and two-dimensionally constrained helium samples, confinement media with very high uniformity and low thermal conductivity are required.

**Further information:** <http://www.nls.physics.ucsb.edu/best/> ,  
<http://funphysics.jpl.nasa.gov/technical/ltcmp/best.html> .

## ***MISTE: Microgravity Scaling Theory Experiment***

**Scientific Objectives:** The MISTE flight experiment plans to measure a variety of thermodynamic quantities (isothermal susceptibility, heat capacity, and  $PVT$  measurements) throughout the  $^3\text{He}$  liquid-gas critical region. The theoretically expected behavior for the isothermal susceptibility near a liquid-gas critical point is given by [29]

$$\chi_T^* = \Gamma_0^\pm |t|^{-\gamma} \left[ 1 + \Gamma_1^\pm |t|^\Delta + \dots \right], \quad t \equiv T/T_c - 1, \quad (0.8)$$

where  $\Gamma_0^+$  and  $\Gamma_0^-$  are the leading critical amplitudes measured along the critical isochore above the transition and along the coexistence curve below the transition, respectively.  $\Gamma_1^+$  and  $\Gamma_1^-$  are amplitudes of the first correction-to-scaling that apply farther away from the transition. Renormalization group theory [30] predicts a divergence of the isothermal susceptibility with a leading critical exponent  $\gamma = 1.240$  and a correction-to-scaling exponent  $\Delta = 0.5$ . The heat capacity at constant volume follows a similar expression having a leading critical exponent  $\alpha = 0.109$  and different critical amplitudes.

For most ground-based measurements, a gravity-induced density stratification becomes important near the critical point because of the diverging isothermal susceptibility. These gravity effects have precluded detailed experimental studies in the asymptotic region [31]. This is the motivation for performing critical point measurements in a space environment. These microgravity measurements, performed along various paths (critical isochore, critical isotherm and coexistence curve) can determine the leading critical amplitudes and universal exponents that describe the way thermodynamic properties are predicted to diverge. These microgravity results will self-consistently test asymptotic equation-of-state predictions for universal critical amplitude ratios and relations between critical exponents. Furthermore, the results of these microgravity measurements in the “asymptotic” region very close to the critical point can be used to test equation-of-state models that also describe the “crossover region” farther away from the critical point. These asymptotic and crossover models apply to all simple fluids and fluid mixtures and their unambiguous validation (or modification) will provide a major advancement in condensed matter physics and engineering.

**Experimental Payload:** The MISTE apparatus will consist of a cylindrical experimental cell, Fig.16, positioned so that the residual gravitational field will be pointing along the cell axis. A low temperature valve and sorption pump will be used to change the density in the cell in-situ. High precision measurements of the sample temperature, pressure and density will be made with sensors attached directly to the cell. The cell will be attached to a low temperature probe that is part of the Low Temperature Microgravity Physics Facility (LTMPF). This facility, planned to be on the ISS, will provide the cryogenic environment for the MISTE experiment.

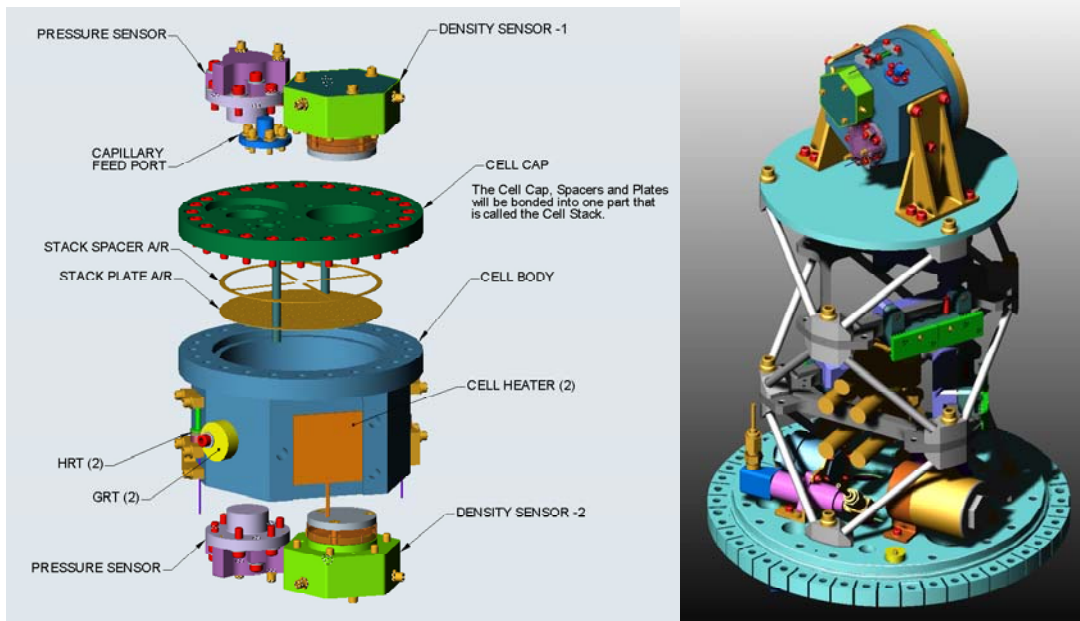


**Figure 16:** The left drawing is an exploded view of the MISTE cell. The cell will have ~ 60 (0.025 cm thick) copper plates and spacers fused together to reduce the thermal equilibration time. There will be two sets of temperature, density, and pressure sensors attached to the cell. The right drawing shows the cell and associated sub-systems attached to the LTMPF low temperature probe support structure.

**Mission Scenario:** The MISTE experiment will require at least 4 months in a micro-gravity environment. Before the flight, the cell will be filled to the critical density. Initial heat capacity, susceptibility and *PVT* measurements will be performed along the critical isochore and coexistence curve. Additional measurements will be performed along several isochores above and below the critical isochore by adding and removing mass from the cell. A guest experiment, Coexistence Boundary Experiment

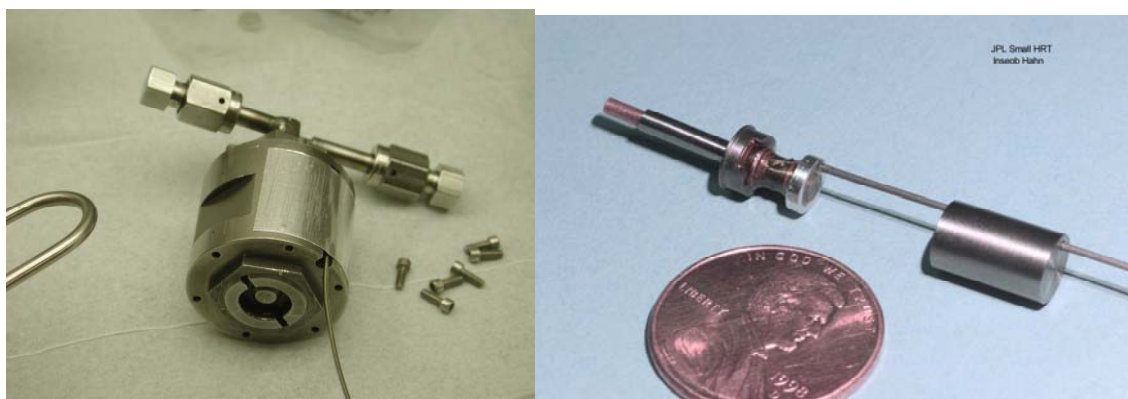


**Figure 17:** The left picture is a small, normally closed low temperature valve developed in collaboration with Mission Research Corporation. The picture on the right is a miniature  $GdCl_3$  high-resolution thermometer that was initially developed specifically for the MISTE experiment.

(COEX), will also perform drift heat capacity measurements to measure the shape of the coexistence curve very close to the  $^3He$  liquid-gas critical point.

**Technology:** The need to change the cell density in-situ required the development of a low temperature valve that can be actuated multiple times, Fig.17. Also, a sensitive

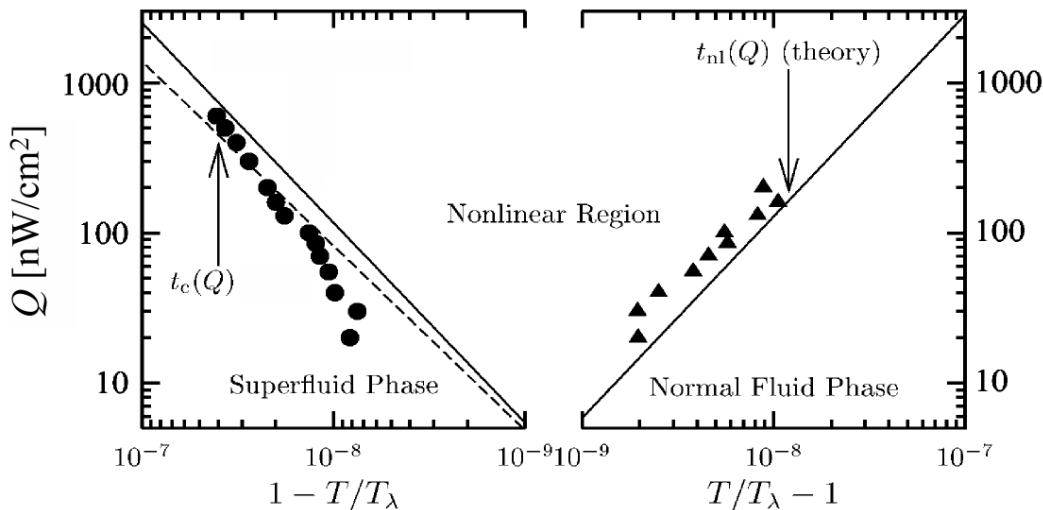
1 nK SQUID-based  $\text{GdCl}_3$  high-resolution thermometer was developed to operate in the temperature range near the  $^3\text{He}$  liquid-gas critical point ( $T_c = 3.315$  K), see Fig.17.

This research was carried out by the Jet Propulsion Laboratory, California Institute of Technology, under contract with the NASA.

**Further information:** <http://miste.jpl.nasa.gov/> ,  
<http://funphysics.jpl.nasa.gov/technical/ltcmp/miste.html>.

### ***DYNAMX: Critical Dynamics in Microgravity***

**Scientific Objectives:** When pure liquid  $^4\text{He}$  is driven away from equilibrium by a heat flux  $Q$  through the liquid its superfluid phase transition evolves from a simple critical point into a fascinating nonlinear region where all transport theories based on linear response fail. Numerous theoretical analyses of this phase transition driven far from equilibrium have resulted in predictions for many new phenomena, including a quasi-scaling relation for thermal profile within the helium's critical region [12], a thermal resistance within the superfluid helium which does not exist in Earth-based laboratories [32], and a depression of the superfluid transition temperature with  $Q$  [13]. Field theoretic renormalization group calculations have predicted the thermal conductivity of helium in this nonlinear region as a function of temperature and heat flux [12]. No hysteresis has been observed in the superfluid transition under a heat flux on Earth, however such hysteresis may occur on orbit [14]. The superfluid / normal fluid interface is predicted to be stable on orbit, but only under a heat flux [33]. The DYNAMX experiment will explore these aspects of the superfluid transition driven far from equilibrium in the weightless environment on the ISS. A guest experiment, called  $\text{CQ}^3$ , will measure the enhancement of the heat capacity of superfluid helium due to the heat flux in the same apparatus. This fascinating nonlinear region, with experimentally determined boundaries, is displayed in Fig.18. Ground measurements, made to confirmed proper operation of new technology for DYNAMX. have also discovered a very interesting new self-organized heat transport



<sup>3</sup> The PI of this experiment is D. Goodstein, Caltech.



**Figure 18:** The nonlinear region near the superfluid transition in  $^4\text{He}$  under a heat flux  $Q$ . This simple static critical point at temperature  $T_\lambda$  opens into a fascinating nonlinear region once the helium is subjected to a heat flux. The experimental data that define this nonlinear region may be found in [35].

**Experimental Payload:** The DYNAMX payload consists of a cylindrical helium sample cell that is designed to support a heat flux  $Q$  along its axis. Three high-resolution thermometers (HRTs) measure the temperature of the helium at their respective positions along the cell's length, with thin copper foils penetrating the stainless steel sidewall of the cell around the cell's circumference at each measurement point. Stray heat sources are controlled at the level of a picowatt, and the HRT resolution is demonstrated at  $100 \text{ pK}/\sqrt{\text{Hz}}$  with a drift rate of less than  $10 \text{ fK/s}$ . Heat is extracted from the cell through a  $2 \text{ kK/W}$  thermal resistance to a cooling stage that is regulated to within  $2 \text{ nK}$  of its operating temperature. The inner radiation shield, which surrounds the cell and cooling stage, is also used to measure the specific heating from charged particles with a resolution of  $0.1 \text{ pW/g}$  to assist in the data analysis of all the LTMPF experiments, in an associated effort called 'Particle Heating Detector (PHD)' (PI S.T.P. Boyd, UNM). The DYNAMX experimental payload is displayed in Fig.19.

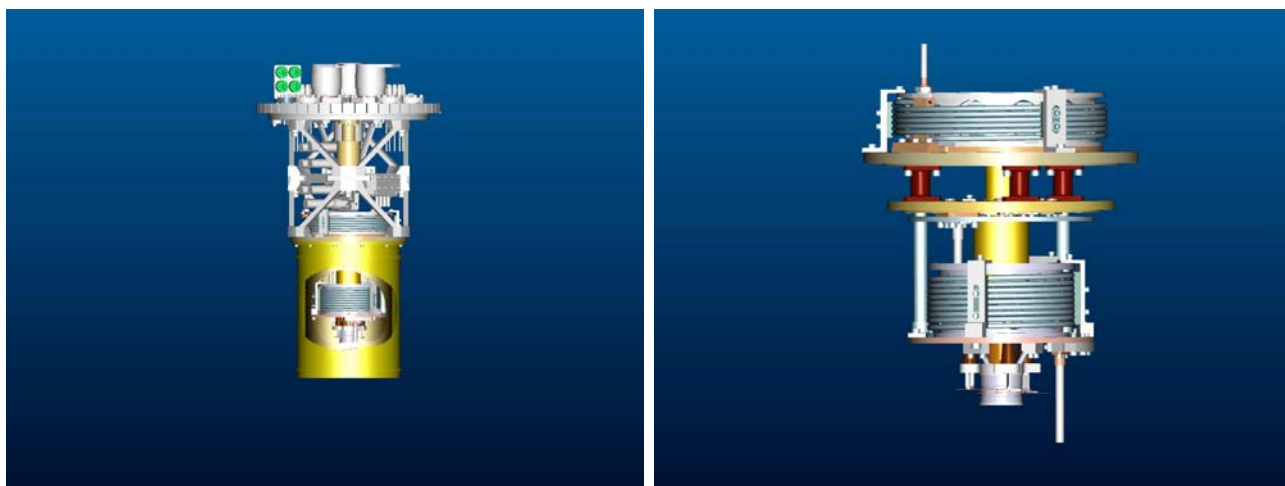


**Figure 19:** The DYNAMX experimental payload, showing the full dewar insert on the left and the cell assembly, with cooling stage and the attach point flanges for the two radiation shields (removed) on the right. This apparatus design includes 107 flight certified component drawings, which are based on laboratory verification through detailed testing on four flight prototypes.

**Mission Scenario:** Once stabilized on orbit DYNAMX will establish a heat flux  $Q$  through the cell and achieve steady state conditions at  $100 \text{ nK}$  below  $T_\lambda$ , and hence in the superfluid phase. Then an additional heat  $\Delta Q = 0.02 \cdot Q$  will be applied to the heated endplate of the cell with only  $Q$  being extracted from the opposite end, causing the cell temperature to increase. A normal fluid / superfluid interface will eventually form at the heated endplate, and advance up the cell very slowly, past each of the three sidewall thermometry probes. The thermal profile measured at each of the sidewall probes will be used along with the interface advance rate to determine the thermal conductivity within the nonlinear helium behind the advancing interface. The

spatial temperature profile measured in this nonlinear region at each  $Q$  over the entire range of  $Q$  ( $5 \leq Q \leq 200 \text{ nW/cm}^2$ ) will be used to test for quasi-scaling, and the variation  $T_c(Q)$  will be compiled, where  $T_c(Q)$  is the temperature where the interface forms. A search for hysteresis will be performed by noting any difference in the temperature when the interface enters the cell versus when it leaves. All measurements will be made under saturated vapour pressure by making these measurements with a trapped helium bubble in a separate chamber outside the heat flux within the cell assembly. The CQ guest experiment will measure the heat capacity of the superfluid as a function of both temperature and heat flux, and use this information to determine if our thermodynamic models of the superfluid are accurate in the critical region. The PHD data will be used to prepare a map of particle heating as a function of latitude, longitude, and altitude throughout the mission, for use by all current and future investigators planning exceptionally energy sensitive experiments for orbit.

**Technology:** A new class of paramagnetic susceptibility thermometers has been developed that utilize a dilute concentration of manganese ions in palladium as the thermometric element. These thermometers have achieved excellent resolution ( $100 \text{ pK}/\sqrt{\text{Hz}}$ ) and low drift ( $< 10 \text{ fK/s}$ ) with a fast time constant ( $15 \text{ ms}$ ), and each thermometer's mass is only  $2.7 \text{ g}$ . A new miniature cryogenic valve has been developed that is superfluid leak tight with a mass of only  $1.5 \text{ g}$ . New cell technology has been designed to provide uniform heat flux across a  $2.5 \text{ cm}$  diameter cell from a point-like heater on a  $5 \text{ mm}$  thick composite aluminium cell endcap. The stainless steel cell wall is only  $75 \text{ microns}$  thick near where the copper sidewall foils penetrate to achieve good thermal contact to the liquid helium within the cell, and small corrections associated with the heat flux perturbations at these sidewall probes are well understood and minimized. Finally, new methods of thermal isolation and control have been developed to obtain the DYNAMX science, and to determine the level of charged particle heating throughout the mission.

**Further information:** <http://coffee.phys.unm.edu/dynamx/>  
<http://funphysics.jpl.nasa.gov/technical/lcemp/dynamx.html>

## ***EXACT: EXperiments Along Coexistence near criTicality***

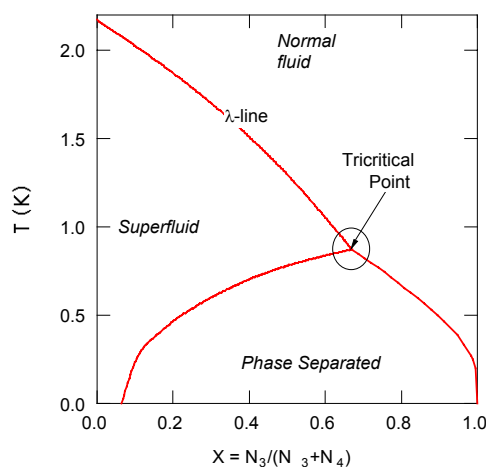


**Figure 20.** The phase diagram of  $^3\text{He}$ - $^4\text{He}$  mixtures in the concentration-temperature plane.

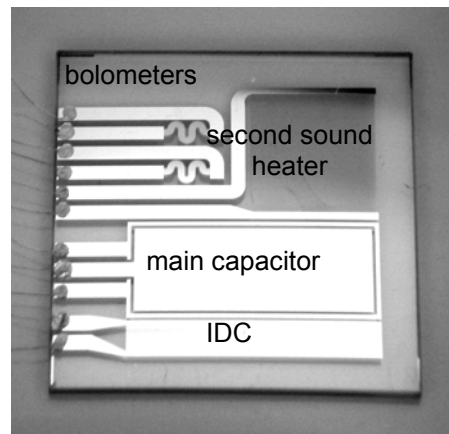
**Scientific objectives:** Over the last 25 years RG theory has been developed to a point where it produces highly quantitative predictions of most facets of critical phenomena. Many of these results are necessarily of an approximate nature, but exact predictions are possible for systems of spatial dimension greater than or equal to the marginal dimensionality of the universality class to which the system belongs. One of the few classes of systems for which this actually occurs in nature occurs are tricritical

points. As a result, the associated critical exponents are expected to be *exact* small integer fractions and the corrections to scaling are predicted to take the form of loga-

rhythms. A tricritical point occurs when a line of second order (continuous) transitions meets a first order phase boundary. A prototypical example is found in the phase diagram of liquid  $^3\text{He}$ - $^4\text{He}$  mixtures. (see Fig.20), where for temperatures above 0.867 K the transition between the normal and superfluid phases is second order while below this temperature the transition is first order.

Experimentally, tricritical exponents have not been measured with particularly high accuracy because of experimental complications caused by either impurities and strains in the sample (for solid systems), or gravitationally induced inhomogeneities (in liquids). As a result, for a class of systems for which we have the best theoretical predictions we lack corresponding precise experimental data. Operating in a microgravity environment can drastically reduce the effects of concentration inhomogeneities, opening up a much larger part of the phase diagram for investigation. The objective of EXACT is to obtain a comprehensive set of measurements of the second sound speed near the tricritical point, from which critical exponents for the superfluid density and the shape of the coexistence curve can be obtained. In addition, from the damping of the second it is possible to obtain information about tricritical dynamics.

**Figure 21** The inside of the experimental cell. The opposite plate has a similar layout. The main capacitor plates are used to determine the over all concentration, the interdigital capacitors (IDC) are sensitive to nucleation of the phase separation at the boundaries.



**Experimental payload:** The experimental cell consists of two 25 mm square quartz plates spaced 200  $\mu\text{m}$  apart. As shown Fig.21, each plate supports a heater and superconducting transition edge bolometer for second sound measurements and capacitor plates to determine the  $^3\text{He}$  concentration. By changing the temperature of a second volume, connected to the cell via a low temperature valve, the mixture concentration can be changed. The cell, enclosed in a temperature controlled shield stage is attached to a secondary cooler necessary to reach temperatures well below the base temperature of the LTMPF dewar.

**Mission Scenario:** It is envisioned that EXACT will operate in a microgravity environment for a period of approximately 100 days during which second sound and phase separation measurements will be made at 30 different concentrations, covering 3 decades in reduced distance to the tricritical point and 4 decades in reduced temperature with respect to the  $\lambda$ -line. In addition, at a few concentrations second sound measurements will be done to a reduced temperature of  $10^{-6}$  to investigate finite size effects.

**Technology:** Because EXACT will operate at temperatures in the vicinity of 0.9 K, well below the temperature of the cryogenic environment, a secondary cooler, a charcoal pumped  $^3\text{He}$  evaporator, is required. A normally closed superfluid tight valve has

been developed to separate the experimental cell from the mixture reservoir. SQUID based High Resolution Thermometry (HRT) technology has been adapted for our temperature range near 0.9K using PdMn as the magnetic medium.

**Further information:**

<http://funphysics.jpl.nasa.gov/technical/ltcmp/exact.html>

## ***Conclusion and Outlook***

In this review we have discussed all of the experiments which are scheduled, or under development, for being performed aboard the ISS. Each of these projects benefits in an essential way from the temporal extension of microgravity conditions that is to be found on the ISS, from its large velocity variations, and locally from the extreme thinness of the Earth's atmosphere. None of these Fundamental Physics experiments could be made to work upon the Earth's surface. We have therefore highlighted the fact that there is a great potential for carrying out Fundamental Physics experiments on the ISS. Indeed, there are many more current ideas concerning how the ISS may be used for Fundamental physics experiments, as can be seen from articles elsewhere in this issue. For example, the gravity-free environment may help in the search for tiny non-Newtonian forces, or be instrumental in improving the accuracy of atomic interferometry experiments.

However, it must be acknowledged also that for some experiments the conditions on-board the ISS are not ideal. In these cases a 'drag-free' flyer which houses the experiments, and which still has to be developed, may prove to be the solution. Such a new physics-facility for the ISS would create the ideal combination of a true microgravity environment without disturbances (residual accelerations, for example) and access to the experimental setup for the purposes of adjustment or control — or for post-mission analyses.

## ***Acknowledgement***

We like to acknowledge the following financial support: G.A., N.A., M.B., R.D., J.L., and N.M. from the NASA Office of Biological and Physical Research; P.L.B. from the AUGER theory and membership grant 05 CU1ERA/3 through DESY/BMBF (Germany); K.G. from the NASA Microgravity program and Penn State University; V.D., H.D., and C.L. from the German Space Agency DLR and the European Space Agency ESA; N.L. from ESA.

## ***References***

- [1] D. Giulini, C. Kiefer and C. Lämmerzahl (eds.): *Quantum Gravity – From Theory to Experimental Search*, Springer Lecture Notes in Physics **631** (Springer Verlag, Berlin 2003).
- [2] C. Lämmerzahl and H. Dittus: Fundamental Physics in Space: A guide to present projects, *Ann. Phys. (Leipzig)* **11**, 95 (2002).
- [3] G. Amelino-Camelia, Fundamental physics in space: a Quantum-Gravity perspective, *Gen. Rel. Grav. (this issue)*.
- [4] K.G. Wilson and J. Kogut, The renormalization group and the expansion, *Phys. Rep. C* **12**, 76 (1974); M.E. Fisher, The renormalization group in the theory of critical behavior, *Rev. Mod. Phys.* **46**, 597 (1974).

- [5] C.M. Will, *Theory and Experiment in Gravitational Physics* (Revised Edition, Cambridge University Press, Cambridge 1993)
- [6] T. Damour, Equivalence Principle and Clocks, in Trần Thanh Vân, J. *et al.*, (eds.), *Gravitational Waves and Experimental Gravity*, (World Publishers, Hanoi 2000).
- [7] V. Privman, A. Aharony, and P.C. Hohenberg, in: C. Domb and J.L. Lebowitz (eds.), *Phase Transitions and Critical Phenomena*, (Academic, N.Y. 1991) Vol. 14, p.1.
- [8] V. Privman (ed.), *Finite Size Scaling and Numerical Simulations in Statistical Systems* (World Scientific, Singapore 1990).
- [9] V. Dohm and X.S. Chen, Recent Progress in the Theory of Finite Size Effects, *J. Low Temp. Phys.*, to be published; ; V. Dohm, The superfluid transition in confined  $^4\text{He}$ : renormalization-group theory, *Phys. Scripta* **T49**, 46 (1993).
- [10] F.M. Gasparini, M.O. Kimball, and K.P. Moonay, The superfluid transition of  $^4\text{He}$ , a test case for finite-size scaling at a second-order phase transition *J. Phys.: Condens. Matter* **13**, 4871 (2001).
- [11] D. Murphy, E. Genio, G. Ahlers, F. Liu, and Y. Liu, Finite-size scaling and universality of the thermal resistivity of liquid  $^4\text{He}$  near  $T_\lambda$ , *Phys. Rev. Lett.* **90**, 025301 (2003).
- [12] R. Haussmann and V. Dohm, Nonlinear heat transport near the superfluid transition of  $^4\text{He}$ , *Phys. Rev. Lett.* **67**, 3404 (1991); *Z. Phys. B* **87**, 229 (1992).
- [13] R Haussmann and V. Dohm, Depression of the superfluid transition in  $^4\text{He}$ : renormalization-group theory, *Phys. Rev.* **B 46**, 6361 (1992); V. Dohm and R. Haussmann, The superfluid transition of  $^4\text{He}$  in the presence of a heat current: renormalization-group theory, *Physica B* **197**, 215 (1994).
- [14] F-C. Liu and G. Ahlers, *Physica (Amsterdam)* **194B - 196B**, 597 (1994); A. Onuki, *J. Low Temp. Phys.* **50**, 433 (1983).
- [15] Mansouri, R. and R. U. Sexl, A test theory of special relativity, *Gen. Rel. and Grav.* **8**, 497 (1977).
- [16] S.K. Lamoreaux, J. P. Jacobs, B. R. Heckel et.al., New limits on spatial anisotropy from optically pumped  $^{201}\text{Hg}$  and  $^{199}\text{Hg}$ , *Phys. Rev. Letts.*, **57**, 3125-3128, 1986.
- [17] H. Müller, S. Herrmann, C. Braxmaier, S Schiller and A. Peters, Modern Michelson-Morley experiment using cryogenic optical resonators, *Phys. Rev. Lett.* **91**, 020401 (2003).
- [18] P. Wolf, S. Bize, A. Clairon, A.L. Luiten, G. Santarelli, and M.E. Tobar, Tests of relativity using a microwave resonator, *Phys. Rev. Lett.* **90**, 1060402 (2003).
- [19] V.A. Kostelecky and M. Mewes, Signals for Lorentz violation in electrodynamics, *Phys. Rev.* **D 66**, 0056005 (2002).
- [20] J.P. Turneaure, C.M. Will, B.F. Farrell et al., Test of the principle of equivalence by a null gravitational red-shift experiment, *Phys. Rev.* **D 27**, 1705 (1983).
- [21] C. Salomon et al., *C.R. Acad. Sci. Paris*, **2**, Série 4, p. 1313 (2001)
- [22] A. Bauch and S. Weyers, New experimental limit on the validity of local position invariance, *Phys. Rev.* **D 65**, 081101(R) (2002).
- [23] K. Gibble and S. Chu, Laser-cooled Cs frequency standard and a measurement of the frequency shift due to ultracold collisions, *Phys. Rev. Lett.* **70**, 1771 (1993).
- [24] C. Fertig and K. Gibble, Measurement and cancellation of the cold collision frequency shift in an  $^{87}\text{Rb}$  fountain clock, *Phys. Rev. Lett.* **85**, 1622 (2000).
- [25] Y. Sortais, S. Bize, C. Nicolas, A. Clairon, C. Salomon, and C. Williams, Cold Collision Frequency Shifts in a  $^{87}\text{Rb}$  Atomic Fountain *Phys. Rev. Lett.* **85**, 3117 (2000).
- [26] R. Legere and K. Gibble, Quantum Scattering in a Juggling Atomic Fountain, *Phys. Rev. Lett.* **81**, 5780 (1998).

- [27] P. Bhattacharjee and G. Sigl, *Phys. Rep.* **327**, 109 (2000); P.L. Biermann and G. Medina-Tanco, Ultrahigh energy cosmic ray sources and experimental results, invited review for the CERN meeting July 2002, in press (2002), *astro-ph/0301299*; P.L. Biermann and G. Sigl, Introduction to Cosmic Rays, in M. Lemoine, G. Sigl (eds.), *Physics and Astrophysics of Ultra-High-Energy Cosmic Rays*, Lecture Notes in Physics 576 (Springer-Verlag, Berlin 2001), p. 1; F. Halzen, The Highest Energy Cosmic Rays, Gamma-Rays and Neutrinos, *Int. J. Mod. Phys. A* **17**, 3432; M. Nagano and A.A. Watson, *Rev. Mod. Phys.* **72**, 689 (2000).
- [28] G. Amelino-Camelia, Giovanni, T. Piran, *Phys. Rev. D* **64**, 036005 (2003).
- [29] D.S. Graywall and G. Ahlers, Second-sound velocity and superfluid density in  $^4\text{He}$  under pressure near  $T_\lambda$ , *Phys. Rev. A* **7**, 2145 (1973).
- [30] F. Wegner, Corrections to Scaling Laws, *Phys. Rev. B* **5**, 4529 (1972).
- [31] R. Guida and J. Zinn-Justin, Critical exponents of the  $N$ -vector model, *J. Phys. A* **31**, 8103 (1998).
- [32] F. Zhong, M. Barmatz, and I. Hahn, Application of minimal subtraction renormalization to crossover behavior near the  $^3\text{He}$  liquid-vapor critical point *Phys. Rev. E* **67**, 021106 (2003).
- [33] R. Haussmann, Heat transport and self-organized criticality in liquid  $^4\text{He}$  close to  $T_\lambda$ , *J. Low Temp. Phys.* **114**, 1 (1999).
- [34] P. Weichman, A. Prasad, R. Mukhopadhyay, and J. Miller, Trapped Second Sound Waves on a Nonequilibrium Superfluid-Normal Interface, *Phys. Rev. Lett.*, **80**, 4923 (1998).
- [35] W.A. Moeur, P.K. Day, F-C. Liu, S.T.P. Boyd, M.J. Adriaans, and R.V. Duncan, Observation of self-organized criticality near the superfluid transition in  $^4\text{He}$ , *Phys. Rev. Lett.*, **78**, 2421 (1997).
- [36] P. Day, W. Moeur, S. McCready, D. Sergatskov, and R. Duncan, Breakdown of Fourier's law near the superfluid transition in  $^4\text{He}$ , *Phys. Rev. Lett.*, **81**, 2474 (1998)
-